Collapse Indicators for Existing Nonductile Concrete Frame Buildings with Varying Column and Frame Characteristics

Siamak Sattar[1], Abbie B. Liel[2]

Abstract

Many existing reinforced concrete moment frame buildings in high seismic regions around the world, including the U.S., were built without adequate seismic detailing. Quantifying the relationship between a set of quantitative parameters, known as collapse indicators, and collapse risk metrics can facilitate efficient identification, classification and retrofit of the most collapse-prone buildings. This paper investigates three collapse indicators: (1) the column-to-beam strength ratio, (2) the ratio of lateral (shear) strengths in adjacent stories, and (3) the ratio of column flexural to shear strength. Each collapse indicator is varied separately through a parametric study of 36 idealized buildings, and nonlinear simulation models are dynamically analyzed for a suite of ground motions to assess the collapse performance. The results establish the relationship between the variation of the collapse performance of the building as a function of each collapse indicator, and identify the range over which variation of the collapse indicator significantly influences collapse performance, as well as upper and lower bounds beyond which the indicator is not significant. The results show that the deficiency associated with the column-to-beam strength ratio and the ratio of shear strengths in adjacent stories can be defined efficiently as the average of the associated values in the components at critical floor/story. For the collapse indicator related to the ratio to column flexural to shear strength, the collapse performance is strongly related to the average values in the critical story, and also the location of the most shear critical columns. The

[1] Research Structural Engineer, National Institute of Standards and Technology, Gaithersburg, MD
[2] Associate Professor, Dept. of Civil, Environmental and Architectural Engineering, Univ. of Colorado, Boulder, CO

study also shows that the gradient of the collapse performance with respect to the three collapse indicators is similar.

Keywords: Collapse indicator; nonductile concrete frame building; column-to-beam strength ratio; column flexure-to-shear strength ratio; collapse assessment.

1. Introduction

One of the primary motivations for seismic assessment of existing buildings is to identify buildings that are so potentially dangerous that they are in critical need of retrofit. Existing nonductile reinforced concrete buildings, which are the focus of this study, may have weak or shear critical columns, wide spacing of transverse reinforcement spacing, insufficient reinforcement anchorage and detailing (such as transverse reinforcement with 90 degree hooks), or vertical and plan irregularities, which make them particularly vulnerable to earthquake-induced collapse [1]. In California, for example, many buildings with these characteristics were constructed before approximately 1980, and most have never been retrofitted [2]. Identifying those buildings that are particularly unsafe, from among the broader class of nonductile concrete buildings, can help decision makers, including building owners and local building officials, to prioritize mitigation actions.

A building's collapse risk can be viewed as a function of a set of building characteristics that impact collapse resistance. These characteristics have been referred to as "collapse indicators" [3]. For example, the ratio of column area to floor area could be considered as a collapse indicator. The underlying idea of the collapse indicator perspective put forward by [3] and others is that the building can be classified as unsafe or worthy of further investigation if the values of certain collapse indicators are too severe. Collapse indicators that have been previously proposed vary in terms of the level of difficulty required for computation, from those that can be obtained during

rapid assessment or visual inspection, to those that require engineering calculation, to those that require a complete structural analysis using software tools [3]. The present study focuses on a subset of the engineering calculation type of collapse indicators. These quantities require calculation of demands and capacities using building drawings, but not nonlinear building analyses [3].

This paper studies collapse indicators for existing nonductile concrete frame structures, focusing on collapse indicators related to column and story strength characteristics. In particular, the study examines how the number or distribution of columns or frame lines exhibiting deficient characteristics, and the degree of severity of the deficiency of any individual column or frame line, affects the building's collapse performance. The relationship between the various collapse indicators and assessed collapse performance yields valuable information about the sensitivity of collapse risk to the collapse indicator, and can be used to determine threshold values of the collapse indicator for identifying particularly vulnerable buildings. In addition, the assessments here can be employed to suggest appropriate metrics for collapse indicators in buildings that have widely varying column and frame line characteristics. This study has the secondary goal of examining the collapse indicator methodology proposed by NIST [3] for a case study set of concrete buildings, and explores the feasibility of this method.

2. Collapse Indicator Evaluation Methodology

This study employs a methodology for evaluating collapse indicators that was proposed by the NIST-funded ATC-76-5 project [3], and further explored by the FEMA-funded ATC-78 project [4], in which the authors participated. This methodology requires development of a suite of buildings and building models with different values of the collapse indicator of interest, but otherwise similar or identical properties.

In this method, each building in the suite is subjected to nonlinear dynamic analyses, in order to develop a collapse fragility curve. A collapse fragility curve is a cumulative probability distribution, defining the probability of structural collapse as a function of the ground motion intensity (here given by the spectral acceleration at the first mode period of the building *Sa(T_1)*, *i.e.* $P[Collapse\ |Sa(T_1)]$). Different metrics may be used to quantify collapse performance or risk. One metric of collapse risk corresponds to the ground motion intensity or excitation level at which *50%* of ground motions cause collapse, *i.e.* the median collapse capacity (e.g. [5]), which is denoted here as $Sa_{50}(T_1)$.

After assessing the collapse performance of a building with the particular value of a collapse indicator of interest, the same process is repeated for buildings with different values of the same collapse indicator, in order to explore the trend between the collapse indicator value and collapse performance. Fig. 1a shows a schematic of collapse fragility curves obtained through this process. In Fig. 1b, the variation in the median collapse capacity as function of variation in the value of the collapse indicator is illustrated. Likewise, Fig. 1c illustrates the variation of the probability of collapse conditioned on a specific hazard level varies with the collapse indicator value. Fig. 1b and c are developed from the same collapse assessments in Fig. 1a, but represented using different metrics.

These trends can be used to quantify critical values for each collapse indicator. These critical values serve as a potential threshold distinguishing between buildings that are most at risk of earthquake-induced collapse and those that exhibit smaller risk. One approach for identifying critical collapse indicator values, which is proposed by NIST [3], defines the critical value of collapse indicator where a drastic change is observed in the probability of collapse for a small change in the collapse indicator. The collapse indicator value where the sudden change in the

response occurs is referred to here as the "kink point", and used in this study to show the practicality of this method of identifying the critical collapse indicator. The highlighted region in Fig. 1c shows the range of the identified collapse indicator in which a rapid change in the collapse performance is observed. This region indirectly provides information about the effect of a retrofit; for example, if the collapse indicator measured for a building is close to its corresponding kink point, modestly addressing the deficiency may significantly increase the collapse capacity. However, not all collapse indicator trends will indicate a clearly defined kink point, complicating the use of this point in identification of threshold values. This study does not aim to introduce a threshold value for the kink point for each collapse indicator, instead introducing a range of the collapse indicator at which the most significant change in the response is observed, as shown in Fig. 1c. Alternatively, the critical collapse indicator value could be defined at some pre-defined acceptable probability of collapse. For illustration, a 30% probability of collapse is taken as an acceptable collapse level for identifying the critical value of the collapse indicator in Fig. 1c. Comparison of the actual collapse indicator value in a building to the critical collapse indicator value indicates how much improvement is required to achieve acceptable performance. Of course, the definition of an unsafe building depends on judgment about acceptable risk. This study focuses on identifying the trends between collapse indicators and collapse performance, without presupposing any particular judgment about acceptable level of risk, but with the idea that results could be used in a decision-making context.

When conducting the collapse indicator methodology, variation of the collapse indicators in different models may be accompanied by a change in the strength of the building due to correlations between the collapse indicators of interest and lateral strength. Obviously, strength is significant in building seismic response, and changes in strength may drown out trends in some of

the other, more subtle, collapse indicators. To separate the effects of lateral strength and the collapse indicators of interest here, ground motion intensities are normalized with respect to the maximum shear strength of the building, V_{max}, computed from the peak strength observed during pushover analysis of the building model. (V_{max} can also be computed from a simplified method developed in the ATC-78 project [6], which enables computation of building strength using hand calculations without the need to develop a nonlinear model.)

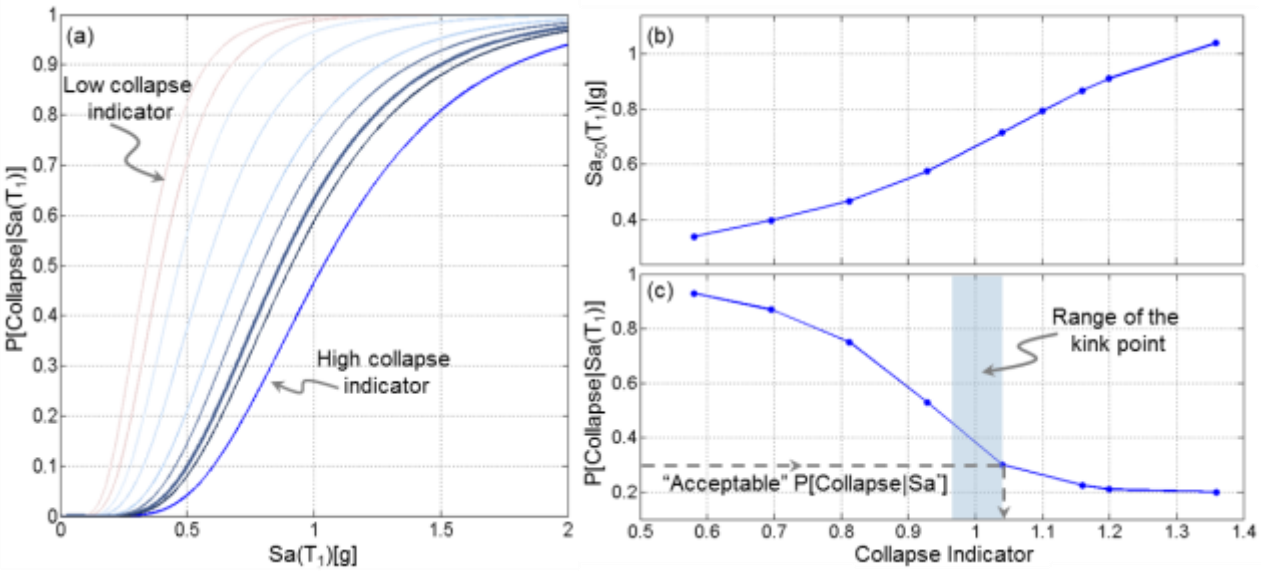

Fig. 1. Schematic illustration of collapse performance as a function of a collapse indicator showing: (a) fragility curves for variation of a collapse indicator in otherwise identical building models; (b) variation of median collapse capacity, as a function of the collapse indicator, and (c) variation of conditional probability of collapse on a specific hazard level, as a function of the collapse indicator.

Accordingly, we employ a normalized measure of ground motion intensity:

$$M = \frac{Sa(T_1)}{V_{max}/W} \quad (1),$$

which can be interpreted as a demand to capacity ratio (and transforms the x-axis of the fragility curve to *M)*. We quantify the collapse performance of the structure by $Sa_{50}(T_1)$, the median collapse capacity in units of g, divided by the ratio of V_{max} to the weight of the structure, W:

$$M_{50} = \frac{Sa_{50}(T_1)}{V_{max}/W} \quad (2)$$

Buildings with higher M_{50} have greater collapse capacity (are able to withstand greater ground motion intensities relative to their lateral strength).

3. Overview of Collapse Indicator Study

This study aims to develop trends between selected collapse indicators and metrics of collapse performance. Three collapse indicators are examined:

(1) the ratio of column-to-beam-strength (M_c/M_b)

(2) the ratio of story shear strengths in two adjacent stories (V_i/V_{i+1})

(3) the ratio of column flexural-to-shear-strength (V_p/V_n)

Collapse indicator (1) is important because it predicts the distribution of damage over the height of the building and, particularly, whether damage concentrates in beams or columns [7]. Note that we refer here to a ratio of beam to column strength, but the "beam" strength includes slab contributions to moment resistance. Indicator (2) can indicate a large discontinuity in story shear strength between two adjacent stories, triggering a weak-story mechanism [8]. Indicator (3) may be critical because it identifies whether columns are likely to fail in shear, flexure or a combination [9]. These three collapse indicators are selected for this study because they are critical collapse predictors and the corresponding deficiencies are common in typical framing found in older concrete buildings. All three of these indicators are measures of structural characteristics and resistance, which has a crucial influence on collapse assessment. Collapse indicators related to relative stiffness in adjacent stories were not found to be critical in early analysis and are not evaluated here. The other important piece is the demand induced in the building by the earthquake. The impact of demand and seismic effect in relation to the collapse indicator is interrogated through the collapse indicator methodology as described in Section 2.

This study considers variations of collapse indicators that are non-uniform across a story or floor. Three concepts are useful for examining the results for buildings with varying frame characteristics. First, the *extent of the deficiency* is considered as the fraction of deficient components, *e.g.* the number of joints with the deficient weak-column condition compared to the total number of joints in the critical story of interest. Second, *the significance of deficiency* is taken to quantify, for example, how much stronger the beams are as compared to columns at each joint. Third, the impact of the *distribution or location of the deficiency, i.e.* the spatial distribution or location of deficient joints within a frame, on the collapse risk is examined.

To quantify the influence of a collapse indicator on the collapse vulnerability of nonductile concrete buildings, a uniform building that is suitable for parametric studies is designed and a nonlinear model of the building is created in *OpenSees*. Then, each of the three collapse indicators is varied separately to create a large suite of parameterized building models and the variation in collapse performance evaluated. Variation of each of the collapse indicators is conducted for: (a) uniform variation, wherein, for example, all the joints in the floor above the critical story have the same M_c/M_b, and (b) non-uniform variation, wherein, for example, the joints in the floor above the critical story have different M_c/M_b values. To achieve these variations, the moment strength of the beams is varied without changing any of the other building characteristics (*e.g.*, all buildings have the same first mode period ($Sa(T_1)$). In total, 36 building variations are considered in this study.

4. Case Study Buildings for Parameterized Study

The initial case study building considered in this study is a six-story reinforced concrete moment frame building in which all frame lines resist lateral loads. The configuration of the building is loosely based on drawings of a building constructed in the 1960s in Seattle, Washington, with five bays in each direction. The first story height is 13 ft., and the upper stories

are 11 ft. high. Interior and exterior span lengths are 24 and 20 ft., respectively. The building has no infill or structural walls.

4.1 Building Design

The building was designed by the ATC-78 project team [11] to resist base shear equal to 10% of the effective seismic weight of the building. This value was chosen as representative of mid-century U.S. seismic designs for mid-height buildings. For use in the collapse indicator methodology, the building was designed using an idealized approach that leads to uniform column-to-beam moment capacity ratios at every joint and uniform ratios of column flexural-to-shear strength at every column.

The designed building has identical column and beam strengths at each joint (*i.e.*, M_c/M_b equal to 1 at every joint), and the lateral column strengths governed by flexural and shear mechanisms are equal in all columns (*i.e.*, V_p/V_n equal to 1 in all columns). For the baseline case, the column dimensions are 18 in. by 18 in. with #8 bars for longitudinal reinforcement and #4 reinforcement at 4 in. on center for closed hoops. Beam dimensions are 18 in. by 28 in. with #8 bars and transverse reinforcement consisting of #4 bars at 10 or 12 in. on center. Due to its uniform characteristics, the building is suitable for the parametric study that is the focus of this study. These dimensions and reinforcement levels are reasonable, but may not be typical due to the need to satisfy the uniformity requirements as a baseline for the parametric study. To develop the designs for the other buildings for the parametric studies, the number and size of longitudinal bars in beams and columns, and number and spacing of transverse reinforcement in the columns, are chosen to satisfy the desired M_c/M_b and V_p/V_n ratios.

4.2 Nonlinear Modeling and Collapse Simulation

4.2.1 Modeling Concept

For use in the collapse indicator methodology, the frame model needs to be capable of capturing the most important characteristics of earthquake-induced response up to collapse. The two-dimensional nonlinear model of the frame aims to capture different failure mechanisms of beams and columns, including those coming from flexural, shear, and axial responses.

The dominant failure mode of a reinforced concrete beam-column depends on several factors including axial load, reinforcement detailing, aspect ratio, etc. Beams are assumed to be dominated by flexural response. This study adopts criteria defined in [5] and [11] to decide whether columns should be simulated as purely flexural elements, shear or flexure-shear elements. This *a priori* designation of failure modes is convenient in the absence of a robust computationally-efficient modeling technique that can capture flexure, flexure-shear and shear failure modes, one of the grand challenges of earthquake engineering simulation [13]. Moreover, Elwood [14] showed that elements modeled with multiple softening modes (shear and flexural) present non-unique numerical solutions. Under the criteria proposed by Elwood [14] , the ratio of the V_p/V_n is computed first, where V_p is the shear demand corresponding to the development of the flexural strength at both ends of the columns, computed based on expected material strengths, and V_n is the column shear strength computed according to ASCE/SEI 41 [12]. Then, columns with $V_{p/} V_n \leq 0.6$ are simulated with the purely flexural element and columns with $V_{p/} V_n \geq 0.8$ are modeled with the combined shear and flexure-shear model. Fig. 2a shows the modeling scheme adopted for each case, with the detailed features described in more detail below. Two main sets of models are considered in this study. In the so-called “shear” buildings, all the columns have $V_p/V_n \geq 0.8$, while in the “flexural” buildings all the columns have the $V_p/V_n \leq 0.6$, but the specific properties of

different columns in each building may vary. Each aspect of the element models is considered in detail in the following sections.

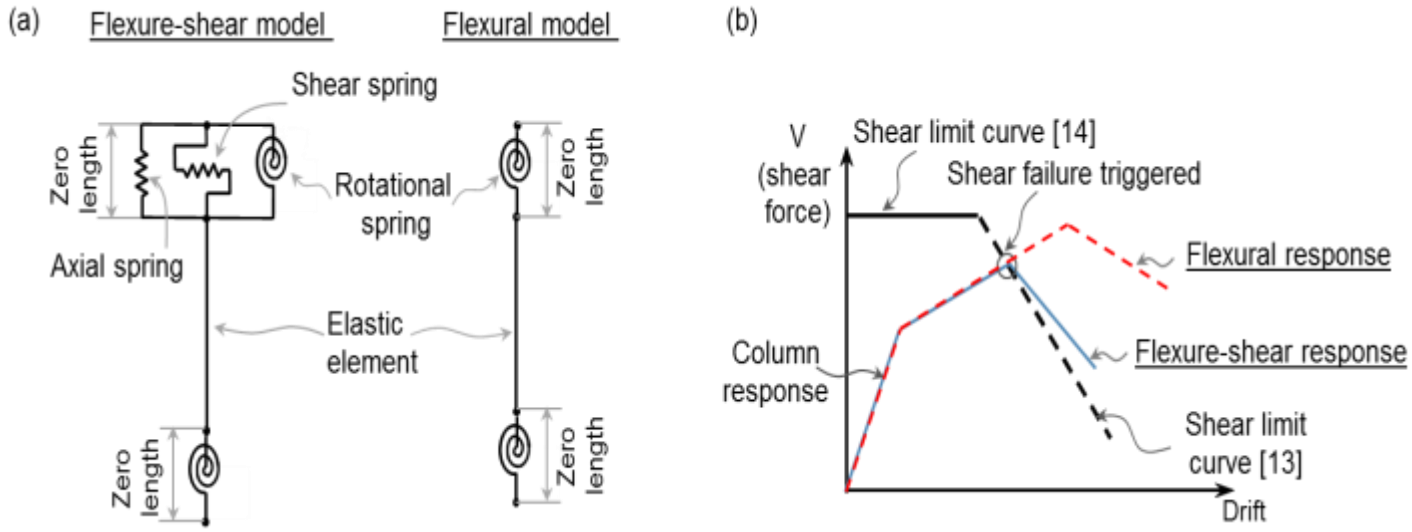

Fig. 2. Illustration of (a) the column flexure-shear model (described in detail in Section 4.2.3 and 4.2.4) and column/beam flexural models (described in detail in 4.2.2) implemented in *OpenSees* and (b) the column flexure-shear and flexural responses.

4.2.2 Modeling of Beams and Columns Failing in Flexure

The flexural response of beams and columns in this study is modeled using the lumped plasticity element model developed by Ibarra *et al.* [16]. The backbone response curve in this model is assigned to the rotational spring in Fig. 2a, and is able to capture the important element flexural response characteristics, as shown in Fig. 2b, including yield strength, ultimate strength, hardening, and softening response, in addition to hysteretic and deterioration properties. An important aspect of this model, which makes it more suitable for modeling flexural-dominated components than fiber-type models in this study because of our focus on collapse, is the post-peak branch of the response which enables the modeling of strain softening of concrete beam-columns, which is caused by the rebar buckling, concrete crushing, and bond failure [5]. Fiber models with softening materials may suffer from a lack of uniqueness in the solution due to localization caused

by strain softening and nonobjectivity with respect to the number of integration points. The Ibarra *et al.* [16] model also captures four modes of cyclic deterioration including stiffness deterioration, strength deterioration due to the hardening and post-peak strain softening, and accelerated unloading stiffness deterioration.

The parameters used to model beam-column elements in this study are computed using a set of equations proposed by [17], which is based on validation of the Ibarra *et al.* model and selected material parameters to 255 reinforced concrete column tests. In this study, these equations were recalibrated based on the subset of the columns that failed in flexure (removing roughly 50 of the tests, which failed in flexure-shear), but utilizing the same functional form. These equations compute the nonlinear modeling parameters as a function of column characteristics, *e.g.* axial load and transverse reinforcement ratio. For this purpose, column axial load is computed from expected (not design) gravity load from dead and live loads. Deformation parameters, such as the rotation capacity, account for bond-slip as well as inelastic deformations.

4.2.3 Modeling of Columns Failing in Shear

If shear failure may occur (either before or after flexural yielding), the response of the concrete columns is modeled based on the shear model developed by Elwood [14] with some modifications. Although work is ongoing by a number of researchers and more data is needed, this model represents one of the most carefully validated models for reinforced concrete column shear failure to date, which is why we adopt it here. Elwood [14] proposed an empirical relationship for a limit curve, which defines the force and displacement at which shear failure occurs in a concrete column, based on a database of 50 experimental tests comprising the vast majority of relevant tests conducted worldwide. Elwood's failure criteria indicate that the position of the limit curve (shown

in Fig. 2b) depends on the transverse reinforcement ratio, axial load, shear stress in the column, concrete compressive strength, and the area of the column.

The shear model initially proposed by Elwood [14] captures only shear failure in columns which first yield in flexure and then fail in shear. To capture brittle shear failure which may occur before yielding, another shear limit curve, based on the shear strength equation proposed by Sezen and Moehle [15], is added to the Elwood model, as shown in Fig. 2b. The shear limit surface from [12] depends on the column's dimensions, transverse reinforcement, axial load, and the concrete compressive strength.

These two limit curves have been implemented in *OpenSees* in the limit state uniaxial material class [14]. The limit state material model traces the response of the beam-column element, and updates the stiffness of the shear spring to a negative value once the response hits the limit curve [14]. This negative stiffness represents stiffness degradation in a column after shear failure occurs.

4.2.4 Modeling of Column Axial Failure

This study adopts the axial failure model developed by Elwood [14] to capture the possible loss of gravity load-bearing capacity that may occur in nonductile concrete columns after shear failure occurs. This model again uses the limit state material model concept to capture the axial failure in the column. Initially, the zero-length axial spring drawn in Fig. 2a is very stiff. The axial limit curve defines the column drift ratio at which axial failure initiates and is a function of column axial load, depth of the column core, and area, yield strength and spacing of the transverse reinforcement. After hitting the axial limit curve, and provided that shear failure has already occurred, and the axial stiffness of the spring is updated with a degraded slope and a residual stiffness. In the Elwood [14] model implemented in *OpenSees*, the response of the axial spring is

coupled to the shear spring through the dependence of the axial response on the shear deformation. This model was developed from a mechanics-based approach, assuming shear failure has occurred, and is appropriate for both a column failing in brittle shear and flexure-shear modes and then failing axially. Models for column shear and axial failure should continue to be improved as more data for columns tested to loss of vertical-load bearing capacity become available (e.g. [13]).

4.2.5 Other Modeling Features

Column and beam models are connected with joints modeled elastically with finite size and elastic response. Here, damping is modeled with a Rayleigh damping value of 2% in the first and the third modes. This damping is assigned only to the elastic elements of the frame, and additional damping comes from the hysteresis of the frame elements. Geometric nonlinearities (P-Δ) are considered in the analyses. The mass of each story is lumped at the floor level and assigned to the nodes at the two ends of the beams. The base of the columns is modeled as fixed.

The modeling approaches adopted in this study for simulation of various actions in each component represent the state-of-the-art for modeling the reinforced concrete moment frames in the performance-based earthquake engineering framework, which requires a compromise between simplicity and accuracy. The buildings designed and modeled do not have an equivalent real building or experiment, and, as a result, the simulated response cannot be validated. The main goal of this study is to provide a defensible relative comparison between the response of buildings with different collapse indicator values to answer questions that cannot currently be addressed by experiments or field data. Results were carefully reviewed by a team of practicing engineers and researchers (see Acknowledgments).

4.3 Collapse Simulation

4.3.1 Incremental Dynamic Analysis

Incremental Dynamic Analysis (IDA) is used to assess the collapse fragility of the modeled buildings [18]. In IDA, a nonlinear structural model is subjected to a recorded ground motion, and dynamically analyzed to simulate the structural response. The time-history analysis is repeated, each time increasing the scale factor on the input ground motion, until that record causes structural collapse. This study uses 44 recorded ground motions (22 pairs) selected to represent large earthquakes with moderate fault-rupture distances (*i.e.*, not near-fault conditions), in order to quantify record-to-record variation in nonlinear structural response. There is substantial literature on ground motion selection and scaling and its influence on structural response predictions, and the record set selected does influence the results [19]. However, these ground motions have been used extensively in FEMA P-695 to develop collapse fragility curves for different buildings such that results can be compared across buildings [20], and are suitable here for relative comparison between buildings.

4.3.2 Collapse Criteria

Different criteria have been proposed to define the occurrence of collapse in a building on the basis of nonlinear analysis results [21]. Most of these collapse criteria identify collapse in a story, since story collapse typically implies global building collapse.

Separate collapse criteria are considered for the building models with columns failing in flexure and shear in this study. For the "flexural" models, collapse is identified if interstory drifts in any story increase without bounds (*i.e.* dynamic instability), as defined in Vamvatsikos and

Cornell [18]. In the flexural models, this limit is consistent with large story deformations, i.e. 12% interstory drift ratio, that cause collapse of one story on top of the one below.

For the "shear" models, two collapse mechanisms are defined here to capture global lateral and gravity collapse modes. (These definitions are similar to those employed by Baradaran Shoraka et al. [21].) The two collapse mechanisms are used as in nonductile frames the critical story is expected to lose its lateral or vertical strength before formation of a sidesway collapse mode.

A global lateral collapse is defined to occur when the shear capacity of a story degrades to less than 40% of that story's maximum capacity, computed as the summation of the maximum lateral strength of all columns in the story. To trigger the global lateral collapse, the capacity of each story is traced by adding the time-varying capacity of columns in that story during the time history analysis. Prior to the triggering of shear failure, the shear capacity of each column is taken as the smaller of Elwood [14] or Sezen and Moehle [15] limit curves (see Fig. 2b). After triggering of shear failure in each column, if the drift in the column is larger than the maximum drift experienced by the column before the point in time in the response history analysis, the capacity of the column is assumed to be equal to the shear demand in that column; in this region of response, the model guarantees that the column follows the prescribed capacity backbone. The cut-off identifying collapse as occurring when the story shear capacity reduces beyond 40% of its maximum capacity is somewhat arbitrary, but the collapse fragility results are not sensitive to the selected value.

Global gravity collapse is triggered when the axial demand on any story exceeds the summation of the axial capacity of columns in that story [21]. For columns in which shear failure has not initiated, the axial capacity is taken as the crushing load of a column. The axial capacity of

a column after initiation of shear failure is calculated from the axial limit curve equation developed by Elwood [14]. The axial demand in each story is constant throughout the analysis and is computed as the summation of the axial forces in the columns in that story from expected dead and live loads.

The collapse identification procedure checks the global lateral and gravity collapse criteria for each story in the building at each time step during the analysis, until one story is identified as being collapsed. The story-based nature of the collapse criteria means that it is the properties of the critical story, or that story in which collapse occurs, that should be represented by the collapse indicator. The case study building always fails in the first story. Therefore, collapse indicators are consistently defined at the first-story level.

5. Results for Column-to-Beam Strength Ratio

5.1 Overview

When a flexurally-dominated frame structure is subjected to intense ground shaking, plastic hinges in columns and beams may form. Column hinging may lead to a weak-story mechanism in which deformations concentrate in a single story [10, 15]. As is well known, formation of hinges in the beams rather than columns allows the building to experience more distributed damage, dissipating more energy, and postponing collapse of the building [7]. As a result, modern seismic design requires stronger columns than beams through the so-called "strong-column-weak-beam" design philosophy [23]–[25]. (For clarity, we note that the use of the word "beam" here refers the bending capacity of the horizontally-oriented elements, considering beams and slab contributions).

However, older concrete buildings may have weaker columns than beams. Although it is well known that as the column-to-beam strength ratio decreases, the likelihood of experiencing a story mechanism increases [5], few studies have examined how variation of column-to-beam strength over the building impacts collapse performance. To study the effect of the column-to-beam moment strength ratio, the collapse indicator M_c/M_b is defined as the summation of the expected moment capacities of the columns framing into each joint, divided by the summation of the expected moment capacities of the beams (and slab) framing into the same joint.

5.2 Uniform Variation of Column-to-Beam Strength Ratio

Our study of the impact of M_c/M_b on collapse capacity is first conducted by uniformly varying the M_c/M_b ratio of all of the joints at the critical floor level, as shown in Fig. 3. The collapse capacity of these buildings is shown in Fig. 4. As expected, the collapse performance of the building increases as the average M_c/M_b ratio at the second-floor level increases; in other words, buildings with lower M_c/M_b ratios are at higher risk of collapse, particularly if $M_c/M_b < 1.0$. Fig. 4 indicates a change in slope on this curve around $M_c/M_b = 1.0$.

Moreover, the results indicate that there are both upper and lower bounds on the range over which M_c/M_b has a substantial impact on collapse capacity. In order to investigate the lower bound in the trend observed between M_{50} and the average M_c/M_b ratio, the collapse performance of models with the uniform M_c/M_b ratio of 0.6, 0.8, and 1.0 in the second floor are compared. Analyses results show that these models have almost the same M_{50} (0.2% difference), while the model with M_c/M_b of 1.0 has a collapse capacity (M_{50}) that is 1.6% larger. This finding implies that the M_c/M_b ratio of 0.8 can be seen as lower bound; at this value, further reduction in the M_c/M_b ratio does not appear to worsen the response of the structure. In order to investigate the upper bound, the collapse performance of three models with M_c/M_b ratios of 1.2, 1.4 and 1.8 are compared. The collapse

capacities of the models with the M_c/M_b ratio of 1.4 and 1.8 in the second floor are almost the same, with 0.8% difference, but 10% larger than the model with the M_c/M_b ratio of 1.2. These results show that as the M_c/M_b ratio increases beyond 1.4, a saturation in the effect of the M_c/M_b ratio occurs; larger M_c/M_b ratios do not further improve the collapse performance of the six-story building.

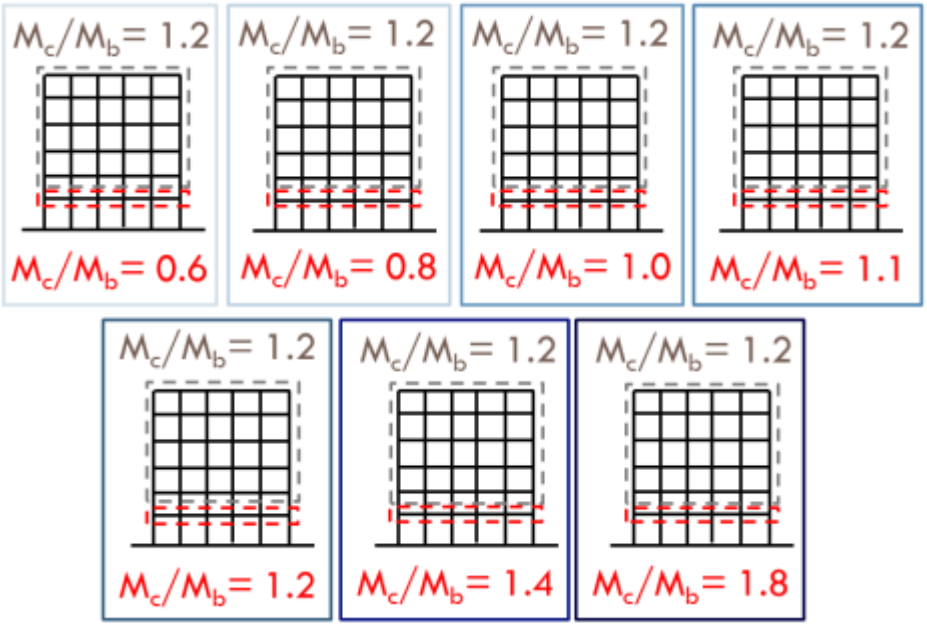

Fig. 3. Schematic drawing of the uniform variation of M_c/M_b ratio of joints in the second floor. In this figure, and similar figures that follow, the dashed boxes identify the M_c/M_b values for all joints within the box.

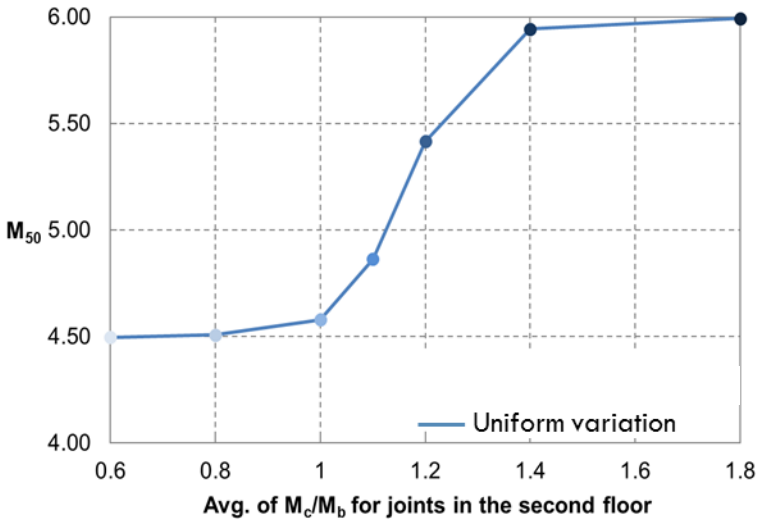

404

405 Fig. 4. Variation of collapse capacity *(M_{50})* of the case study buildings with respect to variation of
406 the average M_c/M_b ratio for joints at the second floor, considering uniform (buildings in Fig. 3)
407 variation in M_c/M_b.

408

409 These bounds are used to propose a new collapse indicator, referred to as the "modified
410 average", in which M_c/M_b at all the joints at the critical floor are averaged, but those joints with
411 M_c/M_b greater than 1.4 are replaced by 1.4, and those with M_c/M_b less than 0.8 are taken as 0.8.
412 This definition is investigated in more detail in the next section through the study of frames with
413 non-uniform variation of this collapse indicator. Fig. 6 replots the analysis results shown in Fig. 4,
414 but with the modified average M_c/M_b on the x-axis.

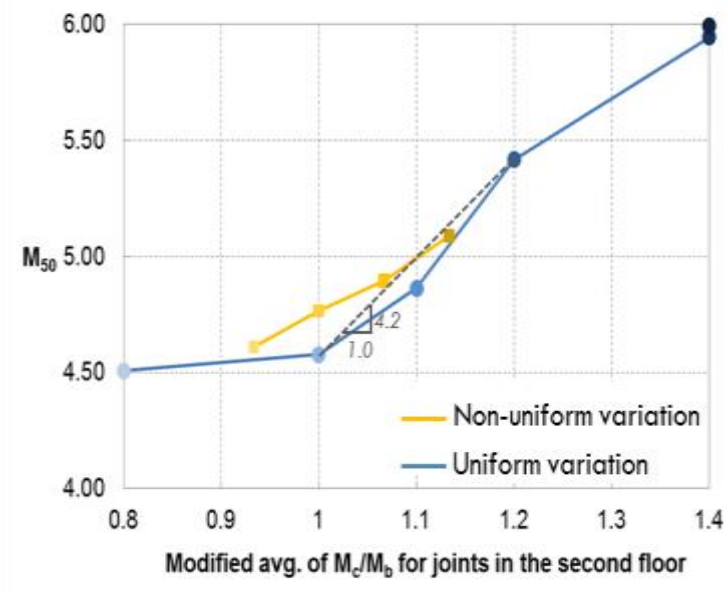

Fig. 5. Variation of collapse capacity *(M_{50})* of the case study buildings with respect to variation of the modified average M_c/M_b ratio for joints at the second floor, considering uniform (buildings in Fig. 3) and non-uniform (buildings in Fig. 6) variation in M_c/M_b.

5.3 Non-Uniform Variation of Column-to-Beam Strength Ratio

5.3.1 Overview

In order to investigate the effect of the variation in the collapse indicator within the frame, a set of building models with non-uniform distribution of M_c/M_b are developed and presented in Fig. 6. The collapse capacity of these buildings is plotted in Fig. 5 with respect to the modified average M_c/M_b ratio in the second floor, and overlaid on the analyses results for the uniform models. As expected, similar to the results observed for the uniform variation of M_c/M_b, the collapse performance of the building increases as the modified average M_c/M_b ratio at the second floor level increases. The marginal differences between the collapse capacities of uniform and non-uniform models are due to the different column collapse sequences in the first story. These differences are investigated in more detail in Section 5.3.3.

5.3.2 Implications for Definition of Global Collapse Indicator

The results in Fig. 5 appear to confirm that the average of M_c/M_b at the critical floor level is a suitable definition for this collapse indicator. Physically, this finding confirms that it is the aggregate ratio of column to beam strengths at a particular floor level that is critical to quantify this story-level phenomenon. To further explore the collapse indicator definition, a collapse indicator based on the minimum value of M_c/M_b is employed as an alternative. Use of the minimum value of a collapse indicator would be appealing if this was a case where a single bad apple, *i.e.* a deficient joint, substantially worsens the behavior. Results show that the minimum definition will predict multiple collapse performance outcomes for buildings with the same value of the collapse indicator. As a result, a collapse indicator based on the minimum M_c/M_b is not an efficient predictor of collapse capacity. Similar results were observed for the case when the maximum value of M_c/M_b of all of the joints at the second-floor level was considered.

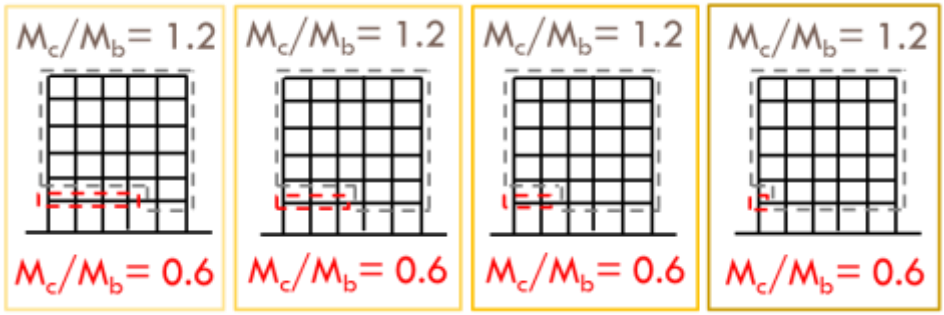

Fig. 6. Schematic drawing of the non-uniform variation of M_c/M_b ratio of joints in the second floor.

The effect of joints with M_c/M_b outside the upper and lower bounds of influence identified by the uniform variation study is further investigated by utilizing two sets of additional models, depicted in Fig. 7. The collapse performance assessments reveal that the three models wherein half of the joints at the critical story have M_c/M_b ratios of 0.4, 0.6, and 0.8 (the three leftmost models in Fig. 7a) have almost the same collapse capacity (0.2% difference), while the model that has three joints with M_c/M_b ratio of 1.0 has a collapse capacity that is 2% larger. Likewise, the

nonlinear dynamic analyses show that the collapse capacity of the models in which three joints have M_c/M_b ratio of 1.4 and 1.8 (Fig. 7b) are the same, and 5% larger than the model in which three joints have the M_c/M_b ratio of 1.2. These findings confirm the bounds identified in above, even when the building geometry is more complex.

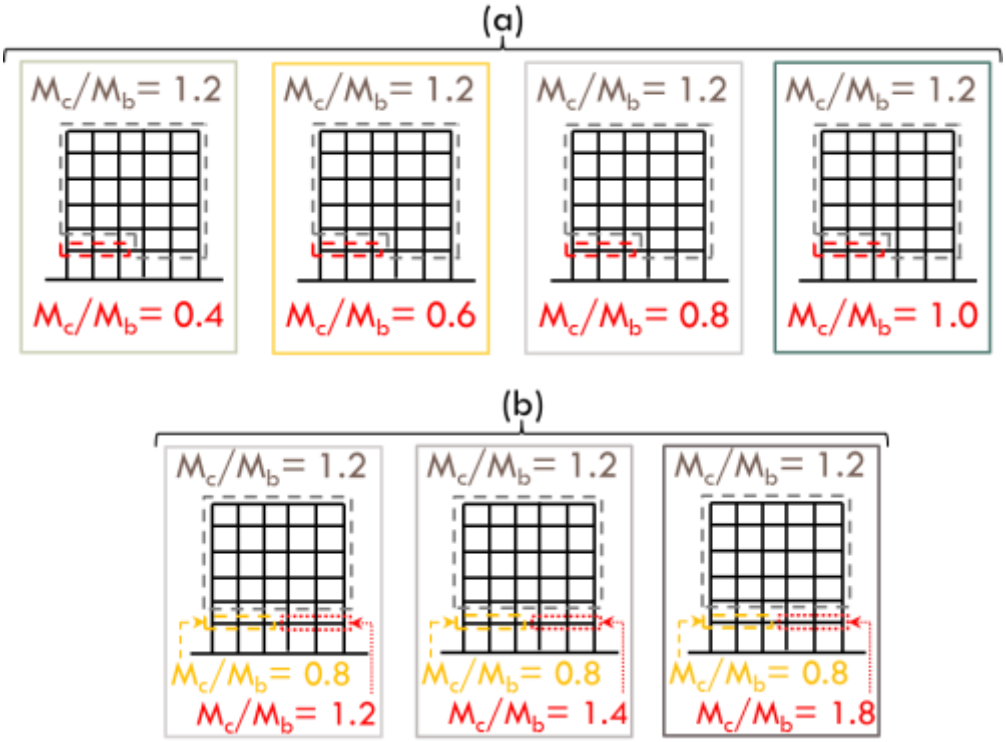

Fig. 7. Schematic drawing for the non-uniform variation of the M_c/M_b ratio in the buildings to find (a) lower and (b) upper bounds.

5.3.3 Extent and Distribution of Deficiency

To investigate the influence of distribution of deficiency in more detail, three cases are considered here and drawn in Fig. 8a-c. For each pair of the models presented in Fig. 8a-c, the modified average of M_c/M_b ratio in the second floor is the same, but the distribution of the deficiency among the joints at the second floor differs.

Fig. 9 shows a maximum difference of 4% in the normalized median collapse capacity results for each pair of buildings. The buildings with non-uniform distribution of M_c/M_b

consistently have slightly higher collapse capacities. This difference occurs because the models that have more variability in M_c/M_b experience more gradual failure, with the columns at the worst joints failing first, while the beams and columns at the better joints are still intact, such that the force can redistribute to the better joints, slightly compensating for the deficiency. Conversely, the collapse of the building with the uniform M_c/M_b ratio in the second floor is sudden, and beams and columns at all joints fail at the same time. However, the overall effect on median collapse capacity is not large.

All of the parametric cases considered so far have examined a building with six column lines or piers. To investigate the effect of the number of piers, a new model composed of two frames in series, connected with rigid links, is tested (Fig. 8d). In this non-uniform model, half of the joints in the second floor have an M_c/M_b ratio of 0.6 and half of the joints have an M_c/M_b ratio of 1.2, such that the modified average M_c/M_b is 1.0. The collapse performance of this model is compared with two other buildings with the same modified average M_c/M_b ratio in Fig. 9, demonstrating that results for the 12-pier frame coincide almost exactly with the results of the single 6-pier frame with non-uniform M_c/M_b ratios. This result provides good indication that the definition of the collapse indicator M_c/M_b is independent of the number of piers or frame lines in the critical story. In addition, we concluded that, since a building with truly uniform joint properties is highly unlikely, and the non-uniform frames show reasonable consistency with the uniform cases, the modified average M_c/M_b ratio in the critical floor is a suitable indicator of collapse performance.

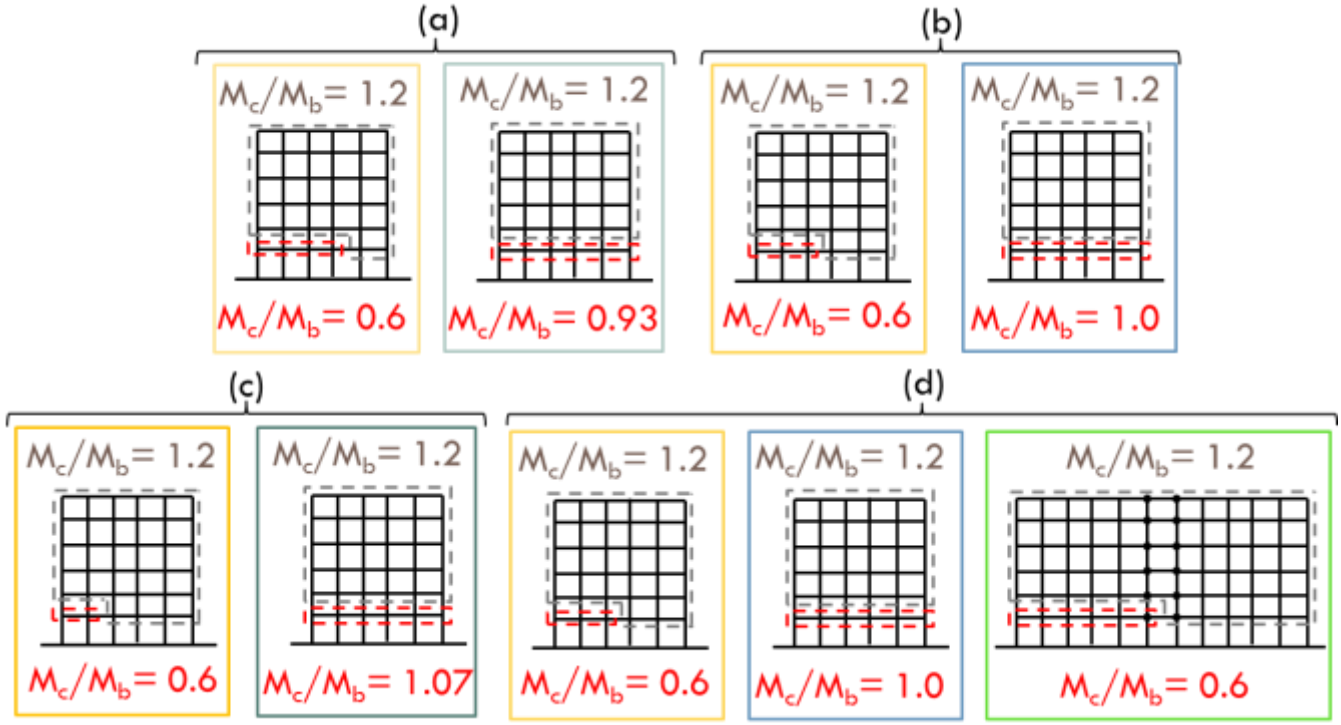

Fig. 8. Schematic drawing of the variation of buildings for studying the effect of the distribution of deficiency M_c/M_b ratio, as well as the number of piers, for buildings with modified average M_c/M_b ratios at the critical (second) floor of (a) 0.93, (b) 1.0, (c) 1.07, and (d) 1.0.

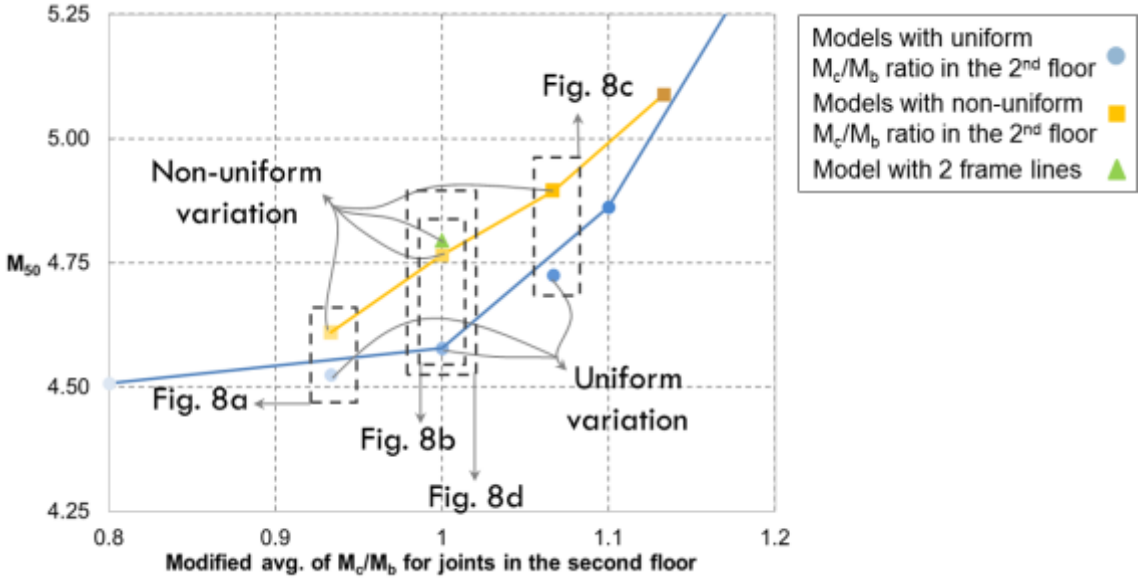

Fig. 9. Comparison among cases with the same modified average M_c/M_b ratio in the second floor, but with different distributions of the deficiency, and different numbers of piers. [Some of the blue and orange points are reproduced from Fig. 5.]

6. Results for Ratio of Lateral Strengths of Adjacent Stories

6.1 Overview

Another common vertical irregularity in older concrete buildings is a discontinuity in story lateral strength between two adjacent stories [3]. This deficiency can lead to weak-story mechanisms, which are characterized by the failure of the building concentrating in one story, with less energy dissipation than a complete collapse mechanism involving formation of plastic hinges over the height of the building [7]. This deficiency may occur anywhere along the height of the structure, but is particularly common between the first story and second stories due to architectural features that tend to make the first story more open. To study the influence of this irregularity, collapse indicator V_i/V_{i+1} is defined in this study, where V_i and V_{i+1} are the shear (lateral) strength of stories i and $i+1$ respectively.

The effect of the variation of V_i/V_{i+1} on the collapse performance of the building is considered using, again, the flexural building models, with the particular interest in buildings with two frame lines which may have distinct V_i/V_{i+1} ratios, and focusing on relative variations in strength between the first and second stories. The V_1/V_2 ratio for the flexural benchmark case study building is 0.85; recall that this building has $M_c/M_b = 1.0$ and $V_p/V_n = 0.6$. To vary the V_1/V_2 ratio, V_1 is adjusted by uniformly varying the moment strengths of the columns in the first story; strengths of beams (at the second floor) were increased accordingly to avoid changing M_c/M_b. The shear strength of each story is calculated as the summation of the lateral strength of all columns in that story.

6.2 Uniform Variation of Ratio of Story Lateral Strengths

To study the effect of V_i/V_{i+1} on the collapse performance of the six-story building, the V_1/V_2 ratio of a two-frame system are varied from 0.6 to 1.4. Initially, each frame has the same V_1/V_2 ratio. The collapse performance of these buildings is plotted in Fig. 10. The variation of the collapse performance of the building is minimal for $V_1/V_2 < 0.9$. In this range, the building consistently experiences the weak-story mechanism in the first story without much deformation in other stories; further weakening the first story (relative to the second story) does not worsen the response. However, as the V_1/V_2 ratio increases up to $V_1/V_2 = 1.2$, the collapse capacity of the building increases. These buildings still experience a first-story mechanism, but as the first-story columns become relatively stronger the building resists a higher lateral demand, in terms of M_{50}, before collapse. For the buildings with $V_1/V_2 > 1.2$, the failure mechanism transfers to the second and third stories, as the first story columns are strong enough to avoid failure in flexure. This change in the failure mechanism explains the descending pattern in collapse capacity observed for models with $V_1/V_2 > 1.2$ in Fig. 10. This finding shows that the performance of the structure suffering from the V_i/V_{i+1} deficiency can be improved by increasing the collapse indicator ratio up to a critical point, but at some point the collapse simply changes mechanism.

6.3 Non-Uniform Variation of Ratio of Story Lateral Strengths

6.3.1 Overview

In order to investigate the effect of variation of the V_i/V_{i+1} collapse indicator for buildings composed of frame lines with different story shear strength ratios, the V_1/V_2 ratio in the two frames are varied separately (i.e. non-uniformly), as shown in Fig. 11. The collapse performance of these buildings is plotted with respect to the average V_1/V_2 ratio of the two frames in Fig. 10. These

results show that the collapse capacities of the buildings with varying V_1/V_2 in different frames lines is similar to the buildings with uniform variation of V_1/V_2, with a maximum difference of 4%.

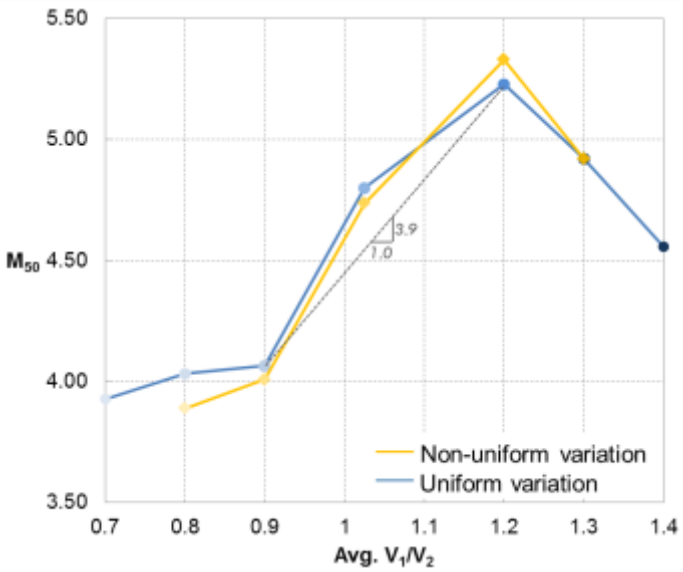

Fig. 10. Variation of collapse capacity *(M_{50})* of the case study buildings with respect to variation of the ratio of first to second story strength, V_1/V_2 considering uniform and non-uniform (models in Fig. 11) variation of V_1/V_2.

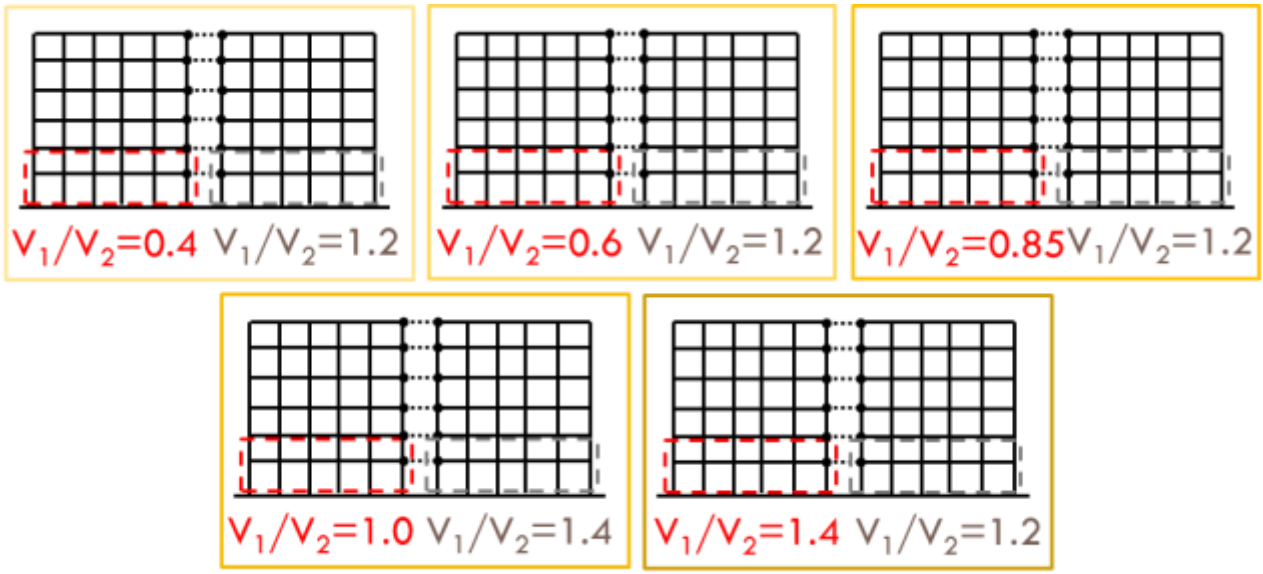

Fig. 11. Schematic drawing of the non-uniform variation of V_1/V_2 ratio of story strengths between frames.

6.3.2 Implications for Definition of Global Collapse Indicator

Fig. 10 suggests that the average of V_i/V_{i+1} between two adjacent stories can be a suitable definition for this collapse indicator, since models with different V_1/V_2 ratios in two frame lines, but the same average V_1/V_2 ratio, have similar collapse capacities. Physically, this finding suggests that it is the aggregate ratio of adjacent story shear strengths among all the frames in the building that is critical, and that load is able to redistribute from the weaker frame to the stronger frame as collapse occurs. In other words, formation of weak story is a story-level phenomenon, and the collapse indicator V_i/V_{i+1} must consider all frame lines, including potentially any gravity-only framing, to quantify this effect.

7. Results for Ratio of Column-Flexure-to-Shear-Strengths

7.1 Overview

Reinforced concrete buildings built before the establishment of modern seismic regulations in 1970s may suffer from various deficiencies in design and detailing, such as wide transverse reinforcement spacing, small bar sizes, or 90 (rather than 135) degree hooks on transverse reinforcement, making the columns susceptible to shear and subsequent axial failure. These failure modes are more concerning than the flexural failures because they can occur in a sudden brittle manner, leading to loss of gravity load-bearing capacity [26]. To measure this vulnerability, the ratio of the flexural to shear strength of columns (V_p/V_n) has been proposed as a collapse indicator [3]. V_p/V_n defines whether the response of a column is controlled by shear or flexure, as well as the degree of shear criticality of a column, *i.e.*, if shear strength of a member is much lower than its flexural strength (large V_p/V_n ratio), the column is expected to fail in shear much before it reaches its maximum flexural strength. To vary the V_p/V_n ratio of the columns, transverse reinforcement

spacing is varied to alter the column shear strength, without any change to the stiffness or flexural strength of the columns. These analyses are all performed with the shear critical column modeling approach, and in frames with $M_c/M_b = 1.0$.

7.2 Uniform Variation of Column-Flexure-to-Shear-Strength-Ratio

To study the effect of the V_p/V_n collapse indicator, the V_p/V_n of columns in the first story are uniformly varied from 0.80 (flexure-critical initially, but may fail in a shear mode after yielding) to 1.20 (highly shear-critical), as shown in Fig. 12. The collapse capacity of these buildings is plotted with respect to the average V_p/V_n ratio in the first story in Fig. 13. As expected, the collapse performance of the building decreases as the average V_p/V_n ratio at the first story increases (i.e. increasing shear criticality in columns). The slope of the variation of M_{50} with respect to V_p/V_n in the most critical region is similar to the observed response for the M_c/M_b and V_1/V_2 collapse indicators.

Fig. 14 illustrates the response of the second pier column in the first story of buildings with columns all having V_p/V_n of 0.8 and 1.2, the two extremes investigated, for a single ground motion record, *i.e.* 1994 Northridge Earthquake recorded at the Beverly Hills station, at the collapse excitation level, up to the time of initiation of the shear failure in the column. Shear failure in the column with $V_p/V_n = 1.2$ initiates at a lower drift ratio, while the column with $V_p/V_n = 0.8$ withstands higher drifts before experiencing shear failure. Due to load redistribution, the shear failure initiation in this column does not correspond with the time collapse occurred in the analysis.

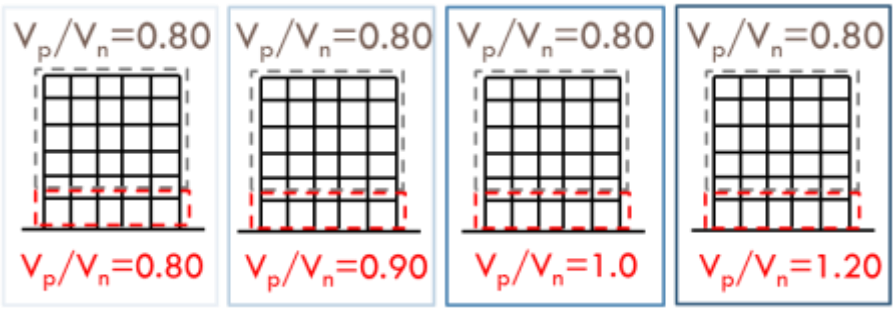

Fig. 12. Schematic drawing for the uniform variation of V_p/V_n ratio in the first story.

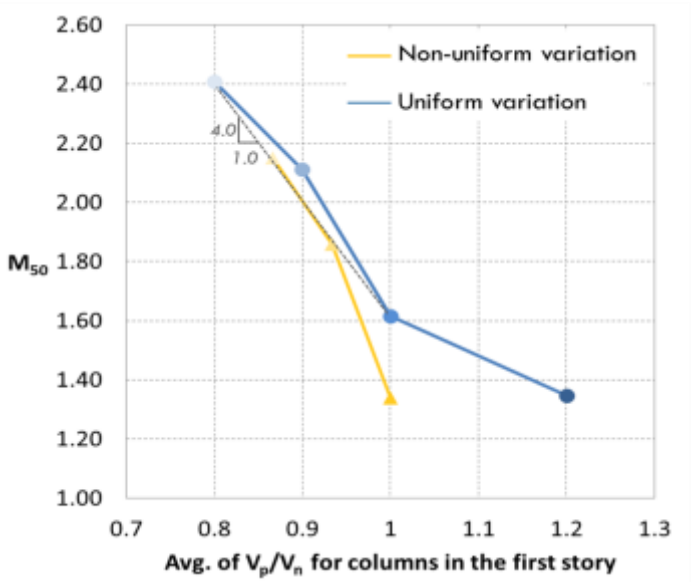

Fig. 13. Variation of collapse capacity *(M_{50})* of the case study buildings with respect to the variation of the V_p/V_n ratio in the first story considering uniform (buildings in Fig. 12) and non-uniform (buildings in Fig. 15) variation of V_p/V_n.

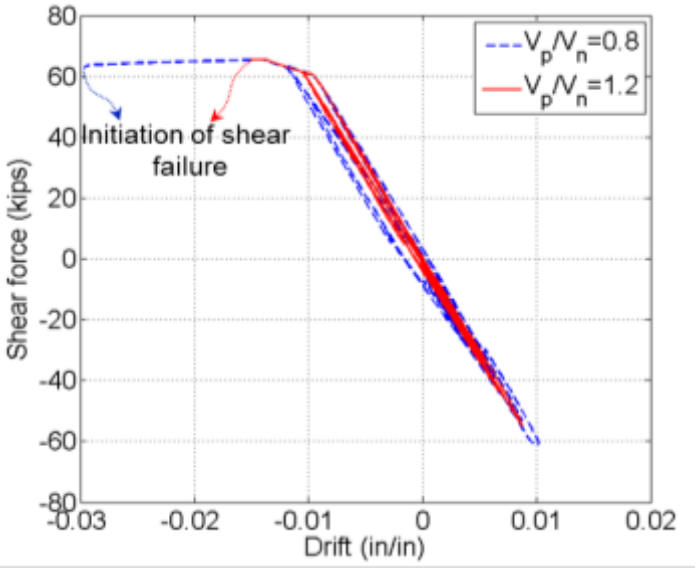

Fig. 14. Variation of the shear force in the second pier column, with respect to the drift of the first story, for buildings with V_p/V_n = 0.8 and 1.2 at the collapse excitation level for the same ground motion (1994 Northridge Earthquake, recorded at the Beverly Hills station).

7.3 Non-Uniform Variation of Column-Flexure-to-Shear-Strength

7.3.1 Overview

To investigate the effect of the non-uniform variation of the V_p/V_n deficiency, the V_p/V_n ratio in the first story is changed by introducing one, two, or three columns with $V_p/V_n = 1.2$, while the rest of columns in the building have $V_p/V_n = 0.8$, as shown in Fig. 15. The collapse performance of these buildings is plotted with respect to the average V_p/V_n ratio in the first story, and overlaid on Fig. 13. The collapse capacities of uniform and non-uniform cases are similar when the average V_p/V_n ratio is considered, although the collapse capacities for the buildings with columns with non-uniform V_p/V_n are 5-17% lower.

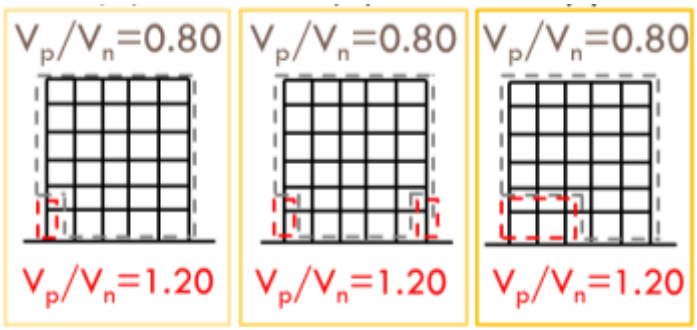

Fig. 15. Schematic drawing for the non-uniform variation of V_p/V_n ratio in the first story.

7.3.2 Implications for Definition of Global Collapse Indicator

To further investigate the appropriate definition of the V_p/V_n collapse indicator, two additional sets of models, depicted in Fig. 16, are analyzed, wherein in each set the number of deficient column(s) is the same, but the location of the deficient column(s) differs. When comparing the two buildings that each have one deficient, *i.e.* shear-critical, column (Fig. 16a), the building with the exterior shear-critical column is shown to have about 40% higher collapse capacity than the one with the shear-critical column at the interior frame line. Likewise, results for the buildings in Fig. 16b demonstrate that the collapse capacity of the models in which two exterior columns have V_p/V_n ratio of 1.2 is 20% greater than the model in which two interior columns have the same extent of shear criticality.

The worse performance of the buildings with shear-critical interior rather than exterior columns is caused by the higher levels of axial load in these columns, since axial load has a direct impact on the drift at which shear and axial failure occurs (both in experimental data and in our models [14]). The buildings with exterior deficient column(s) do not collapse after shear failure of the exterior column, as the other columns in the first story still carry lateral force, and all the columns in that story are resisting the gravity demand. However, in the model with a deficient interior column, shear failure of that column is followed by a drastic loss of the axial capacity

because of its relatively high gravity load demand (axial load ratio of about 0.5). After the axial failure of one or more columns, the analysis can no longer converge because of the inability of the model to redistribute this load. As a result, the model cannot be excited to higher intensity levels. It is noted that some of this effect is a modeling limitation, and the absolute value of the collapse capacity may change slightly with improvement in the solution algorithm and the column shear/axial failure models. However, changes to the modeling are not expected to alter the significance of column location and axial loads in the V_p/V_n assessment.

These observations suggest that the column axial load (due to tributary area and location in the frame) needs to be incorporated in the definition of the V_p/V_n collapse indicator due to the significant axial-shear interactions in reinforced concrete columns. This goal can be delivered by assigning weighting factors in the average calculation, wherein the interior columns get higher weights since they are more important for collapse performance. For example, suppose all of the columns are assigned a weighting factor c_i in the average collapse indicator calculation, and the sum of all c_i is equal to 1. Preliminary analysis, based on the results described above, suggests that if an exterior non-shear critical column has a weighting factor of c, then the exterior shear-critical columns should have a weighting factor of 1.05c, and interior shear-critical columns should have weighting of 5c. This weighted average makes the more shear critical columns more important in the calculation, and put more weight on the shear critical columns with higher axial load. However, these weighting factors should be verified for more cases and under different conditions.

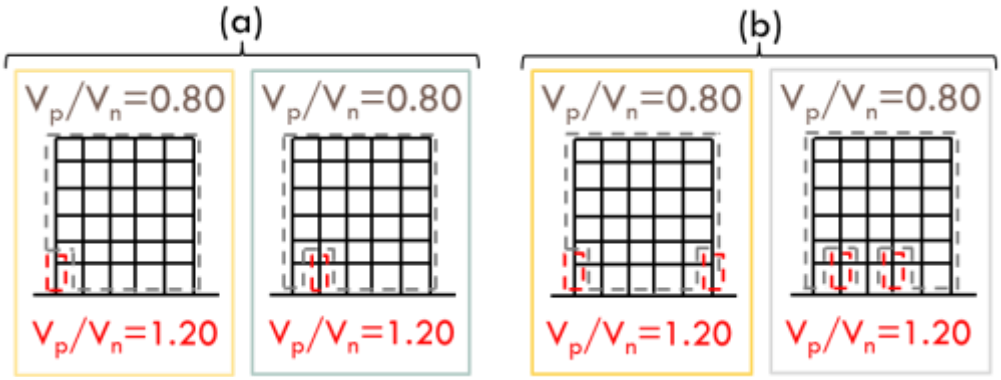

Fig. 16. Schematic drawing for the non-uniform variation of the V_p/V_n ratio to investigate the influence of the location of the deficient column(s).

7.3.3 Significance and Extent of Deficiency

To further investigate the effect of the extent and significance of V_p/V_n deficiency, three more cases are considered here. For each set of models presented in Fig. 17, the average of V_p/V_n ratio in the first story is the same, but the number of the deficient columns, the significance of deficiency, and the number of piers are different. The collapse capacity values for the two models in Fig. 17a are presented in Fig. 18, revealing that the model with uniform V_p/V_n ratio has a 20% higher collapse capacity than the non-uniform model, despite having the same average V_p/V_n. In the non-uniform variation case, the collapse response is dominated by the drift at which a column with V_p/V_n = 1.2 fails. However, in the uniform model all columns have V_p/V_n *=1.0* and shear and axial failure are somewhat delayed, even though the failure of the columns is simultaneous in the four interior columns. Likewise, for the pair of models presented in Fig. 17b, the non-uniform model has an 18% lower collapse capacity than the uniform model. This trend is the opposite of that observed in the M_c/M_b case where the non-uniform variants tended to have slightly higher collapse capacities, due to the more ductile flexural failure mode and the ability of the building to redistribute load from the more deficient to less deficient joints in that case.

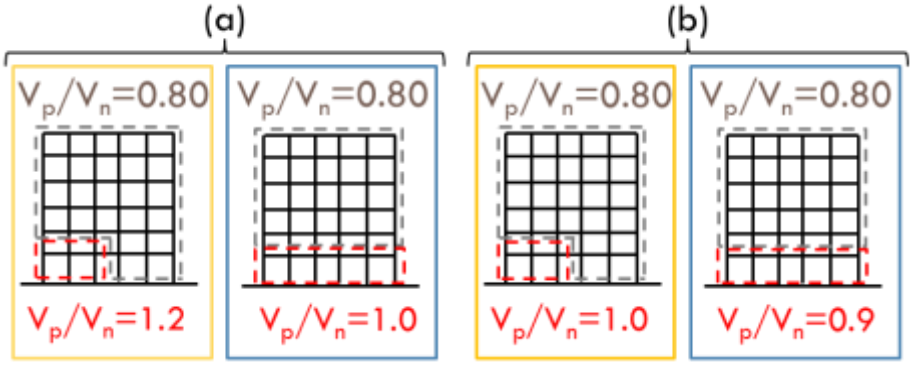

Fig. 17. Schematic drawing for two cases with the same average V_p/V_n, but with different extent and significance of V_p/V_n deficiency.

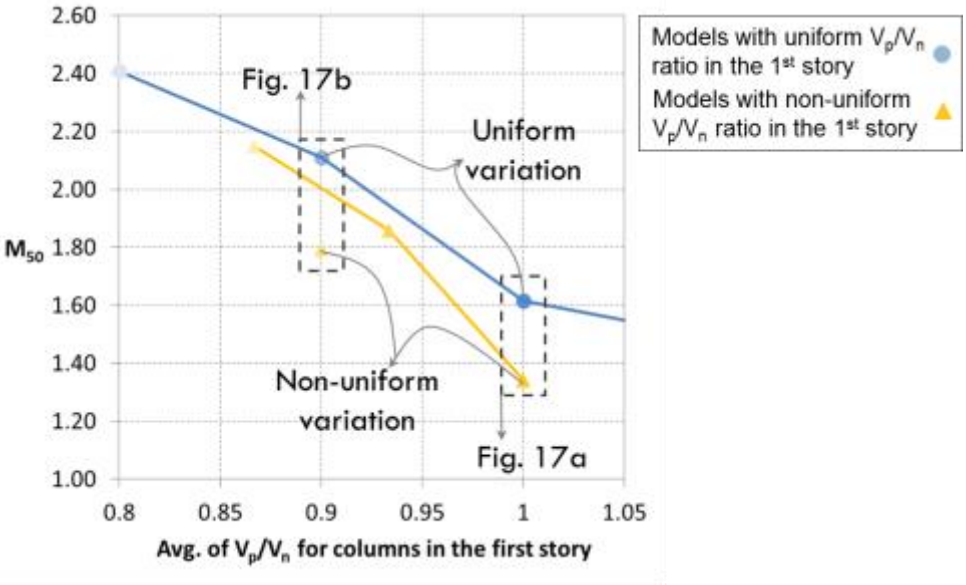

Fig. 18. Comparison among two cases, each having the same average V_p/V_n ratio, but with different distribution of the shear critical deficiency. [The blue and orange curves are reproduced from Fig. 13.]

8. Conclusions

This paper studies the effect of three different collapse indicators for nonductile reinforced concrete frame buildings, specifically, the column-to-beam strength ratio (M_c/M_b), the ratio of lateral strengths in adjacent stories (V_i/V_{i+1}), and the ratio of column flexure to shear strength (V_p/V_n). The study also proposes collapse indicator metrics that effectively capture these three deficiencies in buildings with varying properties from column line to column line. To do so,

673 variation of different collapse indicators in the critical story, *i.e.* the first story, of a six-story
674 building and 36 variants thereof is considered by varying each collapse indicator separately.

675 Findings show the expected decrease in collapse capacity as the average M_c/M_b at the
676 critical floor level decreases. However, the results also demonstrate that there are upper and lower
677 bounds for the M_c/M_b collapse indicator beyond which further enhancing and worsening of the
678 M_c/M_b collapse indicator does not change the collapse performance of the building model. These
679 findings suggest that the M_c/M_b collapse indicator can be defined as the average of the M_c/M_b ratio
680 at the joints at the floor of interest, where the upper and lower bounds are considered in the
681 calculation of the average. The values of the upper and lower bound reported in this study, *i.e.* 1.4
682 and 0.8, likely depend on the number of stories in the building, so more research would be required
683 to define these bounds for cases other than the 6-story building examined here. The results showed
684 that for frames with the same average M_c/M_b, the location of joints with deficient M_c/M_b, as well
685 as the number of column lines in the story, does not significantly affect the collapse performance.

686 Examination of the collapse indicator V_i/V_{i+1} showed that the collapse performance of the
687 building improves as the V_i/V_{i+1} ratio increases. The results confirm that the V_i/V_{i+1} collapse
688 indicator is a story-level deficiency, and can be defined as the average of V_i/V_{i+1} over all frame
689 lines at the floor of interest.

690 The investigation of the collapse indicator V_p/V_n was more challenging. Results confirm
691 that collapse performance of the building is strongly related to the average V_p/V_n ratio in the critical
692 story. However, the distribution of the shear critical columns within a frame, or, in other words,
693 the location of the most shear critical columns, does matter for the collapse performance. This
694 study suggests that a weighted average of column V_p/V_n values, where columns carrying higher
695 vertical (axial) loads are assigned higher weights, may be an effective collapse indicator of shear

criticality in columns. Although advanced shear and axial failure column models were used, this conclusion was made based on nonlinear simulations that involved some convergence issues after shear failure or axial failure occurred in the columns with high axial load.

Finally, results show that the gradient of the collapse performance metric with respect to the three collapse indicators in the critical region is similar. This observation suggests that a relative improvement of each of these normalized collapse indicators has similar impact on the behavior of the structure. The study also suggests that for many collapse indicators, identification of a threshold kink point as envisioned by NIST [3] is impractical, and defining a critical range in which a drastic change in the collapse capacity occurs or thresholds based on relative collapse risk may be more appropriate.

Despite focusing on a six-story building for parametric study, many of the findings of this study are expected to be generalizable to other concrete frame structures. In particular, the proposed definitions of collapse indicators that provide effective predictors of collapse risk are widely applicable, although precise definitions of the upper and lower bounds and weighting procedures may vary with building height or configuration. Nevertheless, other collapse indicators are needed for buildings where other system level deficiencies, such as torsion irregularities, govern the building response. In particular, future research needs to investigate the impact of premature failure of columns or frame lines on one side of the building, which may induce torsion.

For an existing building, decisions about retrofit depend on how deficient each collapse indicator is and how practical or cost effective each collapse indicator treatment would be. The M_{50}-Collapse indicator plots provide information on how effective each collapse indicator treatment would be. More work is needed to investigate how combinations of collapse indicators may impact performance.

Acknowledgments

The work presented here was supported by the Federal Emergency Management Agency (FEMA), through the Applied Technology Council (ATC). The authors gratefully acknowledge contributions and suggestions from the ATC 78 Project Management Committee and Working Group, Panagiotis Galanis, Robert Hanson, Jon Heintz, William Holmes, Steven McCabe, Michael Mehrain, Jack Moehle, and Peter Somers. In addition, we appreciate the contributions of D. Jared DeBock, Kenneth Elwood, and four anonymous reviewers.

References

[1] A. B. Liel, C. B. Haselton, and G. G. Deierlein, "Seismic Collapse Safety of Reinforced Concrete Buildings. II: Comparative Assessment of Nonductile and Ductile Moment Frames," *J. Struct. Eng.*, vol. 137, no. 4, pp. 492–502, 2011.

[2] C. Comartin, D. Bonowitz, M. Greene, D. McCormick, P. May, and E. Seymour, *The Concrete Coalition and the California Inventory Project: An Estimate of the Number of Pre-1980 Concrete Buildings in the State*. Final Draft, August, Earthquake Engineering Research Institute, Oakland, CA, 2011.

[3] NIST, "Program Plan for the Development of Collapse Assessment and Mitigation Strategies for Existing Reinforced Concrete Buildings," NEHRP Consultants Joint Venture, NIST GCR 10-917-7, 2010.

[4] ATC, "Evaluation of the Methodology to Select and Prioritize Collapse Indicators," Applied Technology Council (ATC-78), Redwood City, California, 2011.

[5] C. Haselton, A. Liel, G. Deierlein, B. Dean, and J. Chou, "Seismic Collapse Safety of Reinforced Concrete Buildings. I: Assessment of Ductile Moment Frames," *J. Struct. Eng.*, vol. 137, no. 4, pp. 481–491, 2011.

[6] ATC, "Identification and Mitigation of Non-ductile Concrete Buildings (ATC 78)," Applied Technology Council, Redwood City, California, 2012.

[7] T. Paulay, "An Application of Capacity Design Philosophy to Gravity Load Dominated Ductile Reinforced Concrete Frames," *Bull. N. Z. Natl. Soc. Earthq. Eng.*, vol. 11, no. 1, pp. 50–61, 1978.

[8] T. Paulay and M. J. N. Priestley, Seismic design of reinforced concrete and masonry buildings. New York: Wiley, 1992.

[9] M. Baradaran Shoraka and K. Elwood, "Mechanical model for non-ductile reinforced concrete columns," Journal of Earthquake Engineering, vol. 17, no. 7, pp. 937-957, 2013.

[10] PEER, *OpenSees*. University of California, Berkeley, 2010.

[11] P. H. Galanis and J. P. Moehle, "Development of Collapse Indicators for Risk Assessment of Older-Type Reinforced Concrete Buildings," *Earthq. Spectra*, vol. 31(4), pp. 1991-2006, 2015.

[12] ASCE/SEI, Seismic Rehabilitation of Existing Buildings (ASCE/SEI 41-13), American Society of Civil Engineers, Reston, VA, 2013.

[13] M. R. LeBorgne and W. M. Ghannoum, “Calibrated analytical element for lateral-strength degradation of reinforced concrete columns,” *Eng. Struct.*, vol. 81, pp. 35–48, 2014.

[14] K. J. Elwood, “Modelling failures in existing reinforced concrete columns,” *Can. J. Civ. Eng.*, vol. 31, no. 5, pp. 846–859, 2004.

[15] H. Sezen and J. Moehle, “Shear Strength Model for Lightly Reinforced Concrete Columns,” *J. Struct. Eng.*, vol. 130, no. 11, pp. 1692–1703, 2004.

[16] L. Ibarra, R. Medina, and H. Krawinkler, “Hysteretic models that incorporate strength and stiffness deterioration,” *J. Earthq. Eng. Struct. Dyn.*, vol. 34, pp. 1489–1511, 2005.

[17] C. B. Haselton, A. B. Liel, S. T. Lange, and G. G. Deierlein, “Calibration of Reinforced Concrete Beam-Columns for Simulating Seismic Response to Collapse,” *ACI Struct. J.*, (In press), 2016.

[18] D. Vamvatsikos and C. A. Cornell, “Incremental dynamic analysis,” *Earthq. Eng. Struct. Dyn.*, vol. 31, no. 3, pp. 491–514, 2002.

[19] J. W. Baker and C. A. Cornell, “Spectral shape, epsilon and record selection,” *Earthq. Eng. Struct. Dyn.*, vol. 35, no. 9, pp. 1077–1095, 2006.

[20] ATC, “Quantification of Building Seismic Performance Factors (FEMA P695).” Redwood City, California: Applied Technology Council, 2009.

[21] M. Baradaran Shoraka, T. Y. Yang, and K. J. Elwood, “Seismic loss estimation of non-ductile reinforced concrete buildings,” *Earthq. Eng. Struct. Dyn.*, vol. 42, no. 2, pp. 297–310, 2013.

[22] H. Sezen, “Seismic Behavior and Modeling of Reinforced Concrete Building Columns,” Ph.D. Thesis, University of California, Berkeley, Berkeley, CA, 2002.

[23] ACI, ACI 318: Building Code Requirements for Reinforced Concrete. Farmington Hills, MI: American Concrete Institute, 2008.

[24] CEN, “Eurocode 8–Design of Structures for earthquake resistance–Part 1: General rules, seismic actions and rules for buildings,” *Eur. Stand. NF EN*, vol. 1, 1998.

[25] AISC, *Seismic Provisions for Structural Steel Buildings – ANSI/AISC 341-10*. Chicago, IL: American Institute of Steel Construction, 2010b.

[26] J. P. Moehle, K. J. Elwood, and H. Sezen, “Gravity load collapse of building frames during earthquakes,” *S. M. Uzumeri Symposium: Behavior and Design of Concrete Structures for Seismic Performance*, SP-197, S. A. Sheikh and O. Bayrak, eds., American Concrete Institute, Farmington Hills, Mich., 2002, pp. 215-238 2002.